5

Methotrexate and MCM-41 MSNs

Materials
and
Methods

After the first report on the synthesis of MCM-41[1, 2], a number of synthetic methods for MCM-41 have been reported[3]. All these synthetic methods mainly use surfactants and silica to form a supersaturated solution while maintaining the mixture at elevated temperature for selected periods of time.

5.1 Synthesis of Mesoporous MCM-41 MSNs
5.1.1 Materials

Tetramethyl ammonium hydroxide pentahydrate (TMAOH), tetraethyl orthosilicate (TEOS) and cetyltrimethyl ammonium bromide (CTAMBr) were procured from Sigma Aldrich (USA). Hydrochloric acid, sodium hydroxide and ammonia solution were purchased from E-Merck (India). Double distilled water was used, prepared by double distillation glass assembly. Other reagents and solvents were of reagent grade and were used without further purification.

5.1.2 Synthesis procedure

For the present work, following reported procedure[4] was adopted for the synthesis of MCM-41 nanoparticles (MSNs).

Accurately weighed 9.84 g of cetyltrimethyl ammonium bromide (CTAMBr) was dissolved in 67 g of deionized water. It was then stirred on a laboratory stirrer for 5 min. 6.92 g Tetramethyl ammonium hydroxide pentahydrate (TMAOH) was added drop wise to it with constant stirring. The mixture was allowed to stir for 10 min. 6 g of fumed silica was added to this solution under stirring and vigorous stirring was further continued for 1.5h. The resulting gel of composition SiO_2:0.27 CTAB: 0.19 TMAOH: 40 H_2O was heated in a sealed stainless steel autoclave at 383K for hydrothermal crystallization for desired length of period (48h). The product was recovered by filtration, washed thoroughly with distilled water and then dried at 313K for 4h. Surfactant was removed by ignition process in a muffle furnace, heated at 823K, under an air flow for 5h.

5.2 Characterization

The synthesized mesostructured material was characterized by various instrumental techniques, to get important information about different physicochemical features:

5.2.1 Scanning electron microscopy (SEM)

The morphology of synthesized MCM-41 MSNs was examined by scanning electron microscopy operated at an acceleration voltage of 10 kV. The samples were attached to aluminum stubs with double side adhesive carbon tape then gold coated and examined using a scanning electron microscope, Leo 1430 VP-Germany.

5.2.2 Transmission electron microscopy (TEM)

A high resolution electron microscopic image of the mesoporous MCM-41 MSNs was taken with a JEOL JEM- 2100 electron microscope-USA, equipped with a pole piece, operated at 120 kV. The powder samples were grounded softly in mortar and dispersed in ethanol in an ultrasonic bath for several minutes. A few drops were then deposited on 200 mesh copper grids covered with a holey carbon film. The electron micrographs were recorded in electron negative films and in a digital PC system attached to the electron microscope.

5.2.3 FTIR analysis

MCM-41 MSNs (25 mg) was diluted with dry KBr (300 mg) and ground to a finely divided powder, loaded into a 13 mm die, and pressed under 6000 psi pressure for 5 min. to obtain a pellet. This technique avoids excessive grinding which might cause structural degradation. All measurements were performed at ambient temperature to keep the hydration state of the samples constant and to minimize any structural changes. The spectra were recorded in the range of 4000 cm^{-1}-400 cm^{-1} using a Bruker alpha T, Fourier-Transform Infrared Spectrometer- Germany.

5.2.4 Powder X-ray diffraction (XRD)

Mesoporous MCM-41 MSNs was evaluated using an X'Pert- MPD powder X-ray diffraction spectrometer, Philips- Netherland. In all cases, the generator was operated at 40 kV and 30 mA. In order to avoid the problem of illuminated area at low 2u angles, all the samples were measured using the same sample holder. The MSNs samples were scanned from 1 to 9 of diffraction angle (2θ) at scanning speed of 0.02 2θ/5s.

5.2.5 Nitrogen adsorption-desorption isotherm (BET surface analysis)

Nitrogen adsorption-desorption isotherms were determined using a computer controlled Micromeritics ASAP 2010-USA apparatus. Prior to adsorption measurements, the MCM-41 MSNs was degassed under vacuum overnight at 423K. The specific surface area was determined by application of the B.E.T. method[5] to the isotherm.

5.3 Drug-Methotrexate loading in MCM-41 MSNs

Synthesized MSNs were used for dug loading process. MSNs were dried in oven at 100 °C for 30 min in order to remove moisture from the pores. The drug loading was carried out by direct impregnation method. The MSNs was placed as powder into the drug solution of the drug with a given concentration. The drug loading procedure is described below.

In preliminary drug loading procedure, MTX (100 mg) was dissolved in an appropriate solvent (10 ml) and then MCM-41 MSNs (200 mg) was added. The mixture was kept under magnetic stirring at room temperature for 24h and was

left to settle for 2h to allow the sedimentation of the fine precipitate that was collected by filtration. The recovered solid was dried for 24h under vacuum at room temperature and stored at room temperature.

The drug loaded MSNs were analyzed by XRD, nitrogen adsorption isotherm, surface area, FT-IR spectroscopy and DSC analysis. The loading efficiency (LE) within the MCM-41 MSNs was determined indirectly by determining the amount of non-entrapped or non-adsorbed drug, by measuring concentration of methotrexate (MTX) in the solvent and in the washing solutions. The drug loading efficiency was analyzed spectrophotometrically (Shimadzu-1700, Japan) at 306 nm. Suitable dilution factor was applied and the loading efficiency was calculated according to the formula[6] given below.

$$Wt\% = \frac{m1 - \frac{50}{v}CV}{m2 + \left(m1 - \frac{50}{v}CV\right)} \times 100$$

Where, m1 and m2 correspond to the initial mass of MTX and mesoporous materials added into 0.1 M HCl solution. C is the concentration of filtrates diluted in 50 ml volumetric flask, v is sampled volume from filtrates, and V is the volume of 0.1 M HCl solution for drug loading.

5.3.1 Optimization of drug loading procedure
The process of drug loading was optimized with respect to solvent, drug:carrier ratio, temperature, time, and stirring rate.

□Solvent
Solvent optimization involves the use of different solvents for drug loading and was checked for % of drug load. The main selection criterion was that the solvent should give optimum solubility of drug and minimum or no solubilization of carrier and on that basis different solvents were tried. As different solvents give different pH atmosphere so indirectly, optimization of solvents also covers the optimization of pH.

□Ratio of drug and drug carrier
Another important parameter is to select proper ratio of drug (MTX) and drug carrier (MCM-41) for maximum entrapment. Different ratio were tried and checked for drug loading.

□Temperature and time
Temperature and soaking/stirring time are two important parameters which may affect drug loading. Drug loading procedure was carried out at two different

temperature i.e. room temperature and 40°C. Similarly, five different time durations were selected i.e. 6h, 12h, 24h, 48h, and 72h, for drug loading process.

□*Stirring rate*

Rate of stirring also greatly affect the drug loading, hence it is important to optimize the stirring rate. Effect of stirring at higher and normal rate is studied by using magnetic stirrer.

5.3.2 Factorial design for drug loading optimization

3^3 factorial design was used to determine the effect of the three independent factors: the concentration of drug solution, the stirring rate, and drug: carrier weight ratio on the % drug loading of MCM-41 MSNs. Each factor was tested at three levels of low, medium and high, designed as -1, 0, and +1 respectively.

Microsoft Excel was used for multiple regression calculation in order to deduce the factors having significant effect on the formulation properties. Three-dimensional response surface plots and two dimensional contour plots resulting from equations were obtained by the NCSS software.

5.3.3 Evaluation of drug loaded MCM-41 MSNs

Drug loaded MSNs were evaluated by similar instrumental techniques as described in section 5.2.

5.4 *In-Vitro* dissolution study

In-vitro drug release from the MCM-41 MSNs was studied by the rotating paddle method at 50 rpm (Veego dissolution test apparatus– basket type USP), 37 ± 0.5 °C and in sink conditions. Tests were performed in the following dissolution media[7]: simulated gastric fluid at pH 1.2 ± 0.1, phosphate buffer at pH 4.5 ± 0.1, phosphate buffer at pH 6.8 ± 0.1 and simulated intestinal fluid at pH 7.4 ± 0.1. Drug release was monitored for 1h and compared to MTX crystalline powder, the physical mixture and market formulation. Five milliliters of dissolution fluid was removed from the vessel at predetermined intervals and replaced by the same volume of fresh dissolution medium. The samples were filtered through PTFE 0.45 μm filters and MTX content was determined by UV spectrophotometry (λ max = 303 nm for pH 1.2, λ max = 303 nm for pH 4.5, λ max = 374 nm for pH 6.8, λ max = 372 nm for pH 7.4). All experiments were performed in triplicate and the error was expressed as standard deviation.

Results
and
Discussion

The synthesized MCM-41 MSNs were evaluated for its mesoporosity and structural characteristics by different techniques like electron microscopy, DSC, XRD, FTIR and nitrogen adsorption isotherm. The characterization methods are described below.

5.5 Characterization of synthesized MCM-41 MSNs
5.5.1 Electron microscopy (SEM and TEM)
The surface morphology of the samples was observed by taking their SEM and TEM micrographs (Fig.5.1 and 5.2). It could be seen that synthesized MCM-41 MSNs were regular spherical in shape with smooth surface (diameters<20μm). TEM observations revealed the presence of mesoporous structure with a characteristic hexagonal honeycomb pattern arrangement of the channels.
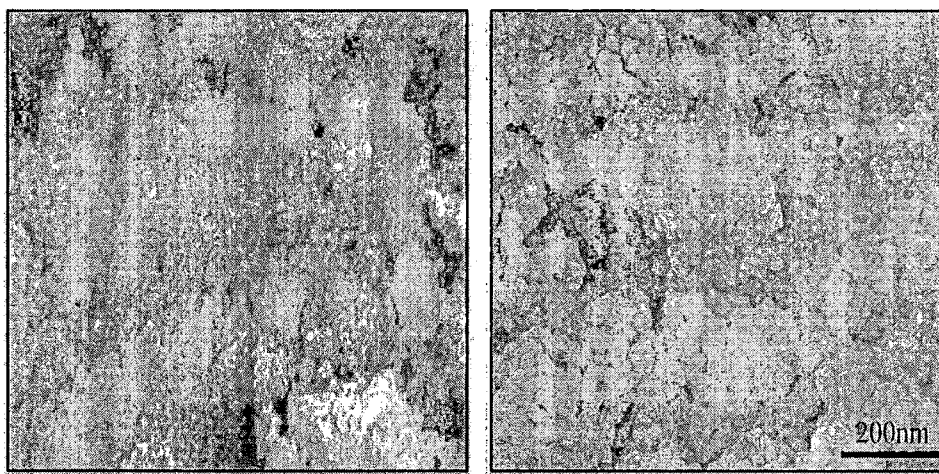
Figure 5.1: SEM images of synthesized MCM-41 MSNs

Figure5.2: TEM images of synthesized MCM-41 MSNs

105

5.5.2 FTIR analysis

Potassium bromide diluted MCM-41 samples were analyzed by FTIR. FTIR spectrum of MCM-41 (Fig. 5.3) showed the presence of a vibration band at 3740 cm^{-1} attributable to isolated terminal silanol groups and of another large band at 3611 cm^{-1} attributable to geminal and associated terminal silanol groups. The stretching vibrations can be seen at 1070 and 958 cm^{-1} for Si-O-Si and Si-OH respectively[7].
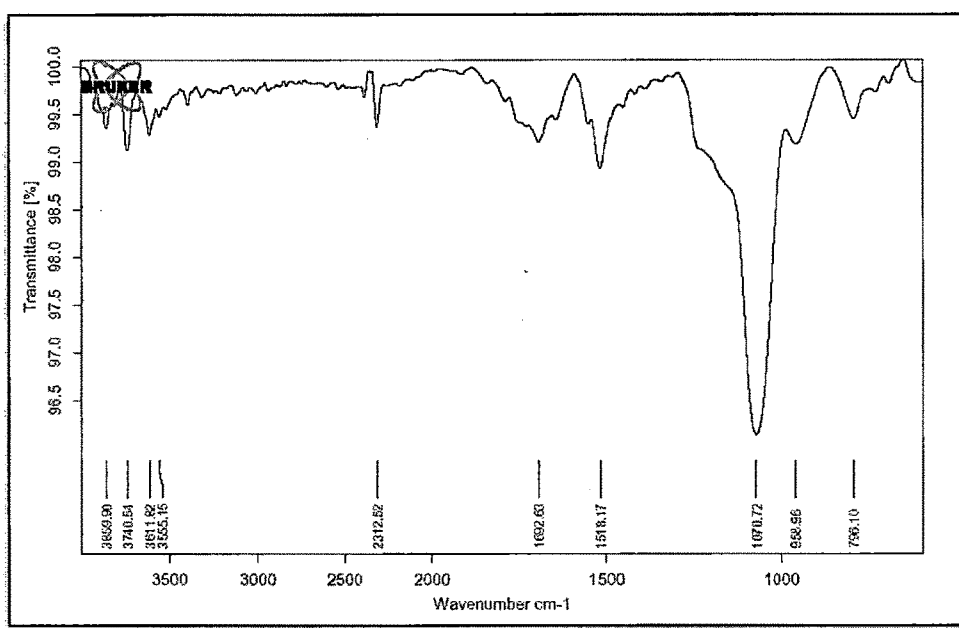
Figure 5.3: FTIR spectra of synthesized MCM-41 MSNs

5.5.3 Powder X-ray diffraction (XRD)

The MSNs samples were scanned at diffraction angle (2θ) from 1 to 9 of at scanning speed of 0.02 2θ/5s. Small angle XRD pattern of MCM-41 MSNs is shown in Fig. 5.4. MCM-41 MSNs diffractogram showed typical reflections[8, 9] between 2° and 9°. It can be seen that XRD pattern of MCM-41 MSNs presents a strong (100) diffraction peak with two small (110) and (200) diffraction peaks, confirming the uniform pore channels and the formation of highly ordered 2D hexagonal mesostructures. The diffraction data of synthesized MCM-41 is in accordance with the reported data[8, 9] for standard MCM-41.
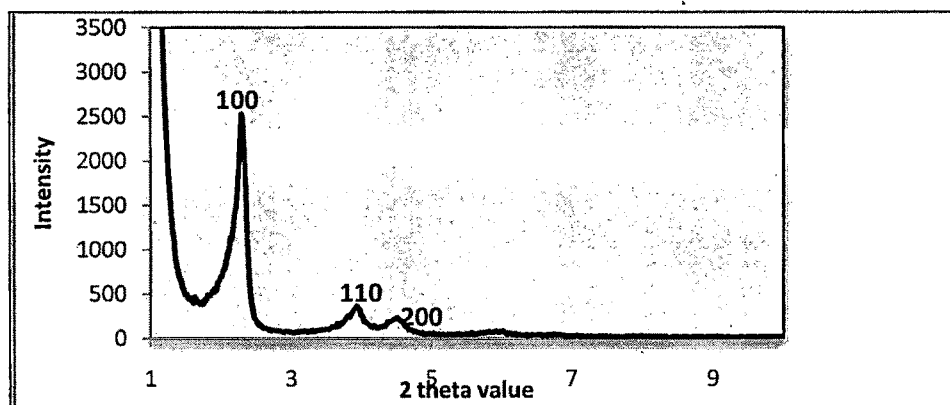
Figure 5.4: XRD of synthesizedMCM-41 MSNs

5.5.4 Nitrogen adsorption-desorption isotherm (BET surface analysis)

Prior to adsorption measurements, the MCM-41 MSNs was degassed under vacuum overnight at 423 K. The inflection of the capillary condensation observed at a P/Po value of about 0.8 for the adsorption isotherms.
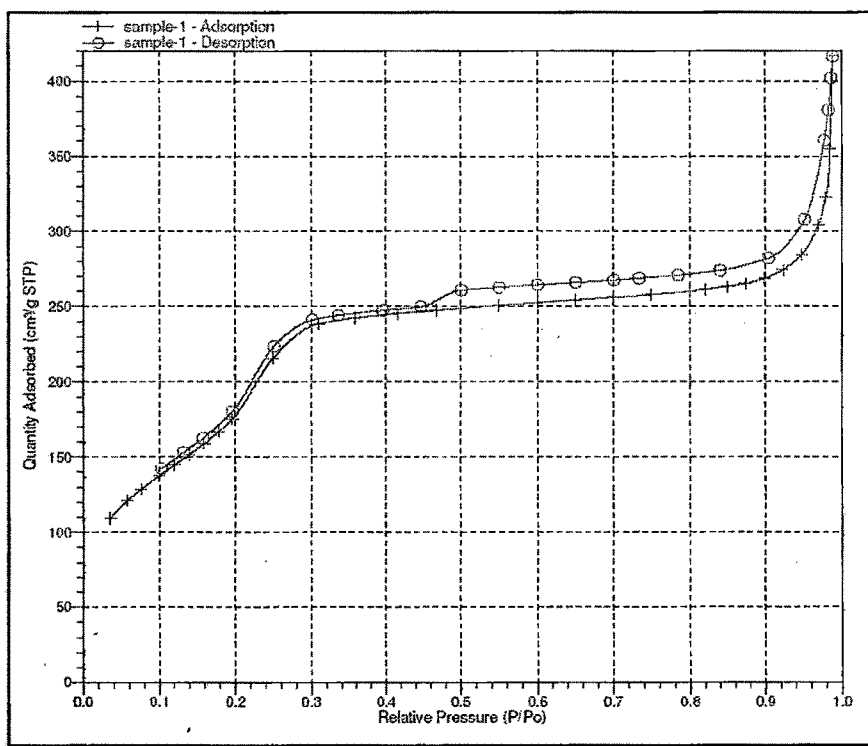
Figure 5.5: Nitrogen adsorption/desorption isotherms of MCM-41 MSNs
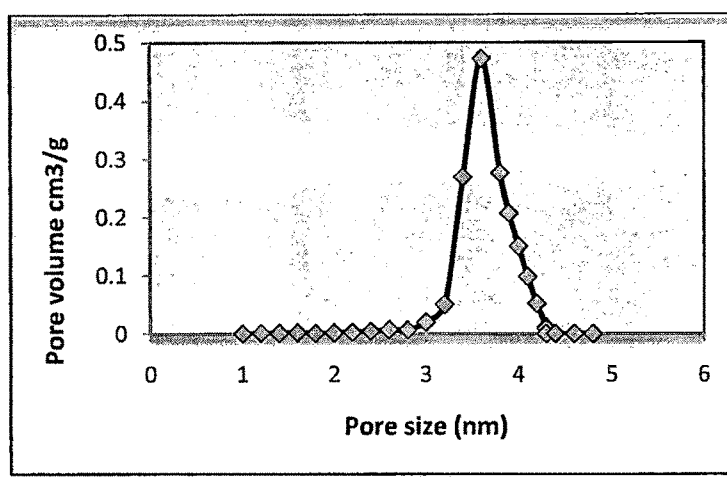
Figure 5.6: Pore size distribution of synthesized MCM-41 MSNs

Table 5.1: Pore diameter, volume and BET surface area of MCM-41 MSNs

MSNs	Pore diameter (nm)	Pore volume (cm^3/g)	S_{BET} (m^2/g)
MCM-41	3.696	0.470	739.671

Nitrogen adsorption-desorption isotherms and pore size distribution of MCM-41 MSNs are shown in Fig. 5.5 and 5.6. Synthesized MCM-41 MSNs shows typical type IV isotherm according to IUPAC classification represents the mesoporosity of the nanoparticles. The isotherm recorded for MCM-41 MSNs also shows a hysteresis loop at high relative pressure, which has been ascribed to the presence of interparticle porosity[5, 10]. The calculated B.E.T. specific surface area for MCM-41 was 739 m^2/g. The average pore size distribution and mesopore volume for MCM-41 MSNs was found to be 3.69 nm and 0.47 cm^3/g respectively. Numerical data is shown in Table 5.1.

5.6 Drug-Methotrexate loading in MCM-41 MSNs

Due to the high specific areas and pore volumes of MSNs, large quantities of drug can be incorporated into the porous MSNs by adsorption to the pore or/and surface of MSNs. The MCM-41 MSNs were added to a concentrated solution of the MTX and the suspension was stirred for about 24h for maximum diffusion of the drug molecules into the mesopores (Fig. 5.7).
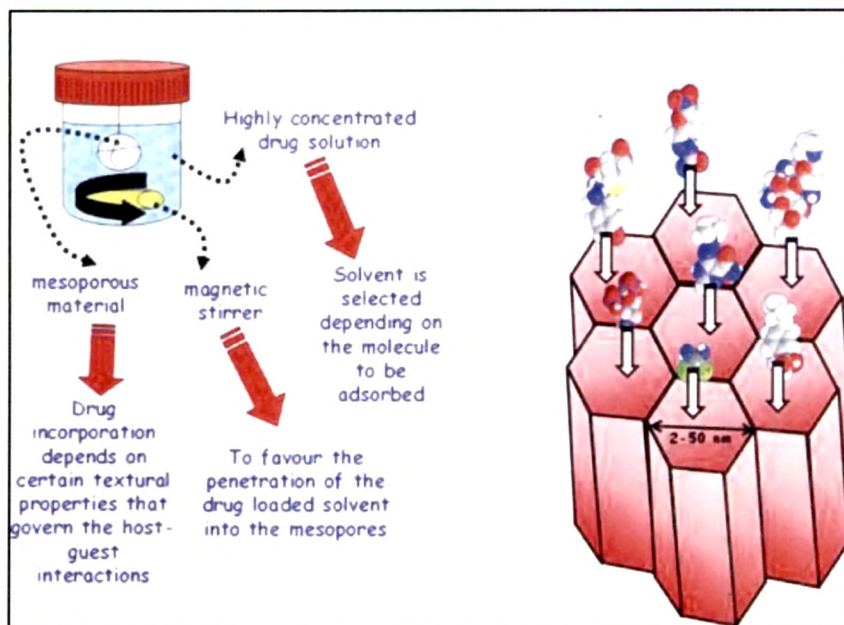
Figure 5.7: Schematic representation of the drug loading procedure

Several factors need to be optimized to achieve maximum drug loading. The right pore size of the synthesized MCM-41 MSNs is important as it determines the size of the molecules which can be adsorbed into the mesopores.

It is important to know whether drug molecules are adsorbed in the pores or on the surface of MSNs as it can later on affect the release characteristics. Normally, pore/drug size ratio>1 allows the adsorption of drug inside the pores[11]. It is reported that the molecular size of MTX is ~ 2.3 nm[12] and the data of nitrogen adsorption isotherm indicated the pore size of MCM-41 MSNs as 3.6 nm giving the pore/drug size ratio as 1.56, indicating that, MTX molecules can be adsorbed in the pores of synthesized MCM-41 MSNs.

The drug loading into the MCM-41 MSNs is also controlled by the chemical nature of the pores and pore walls. The inorganic networks of MCM-41 MSNs have plenty of silanol groups (Si-OH), present into the mesopores and on the surface (Fig. 5.8) that would interact (through hydrogen bond) with the functional groups of the drug[11, 13]. Attracting interaction between the silanol group of MSNs and functional group of the drug, the drug molecules either confined within the pores or they adsorbed to the surface of MSNs[11].
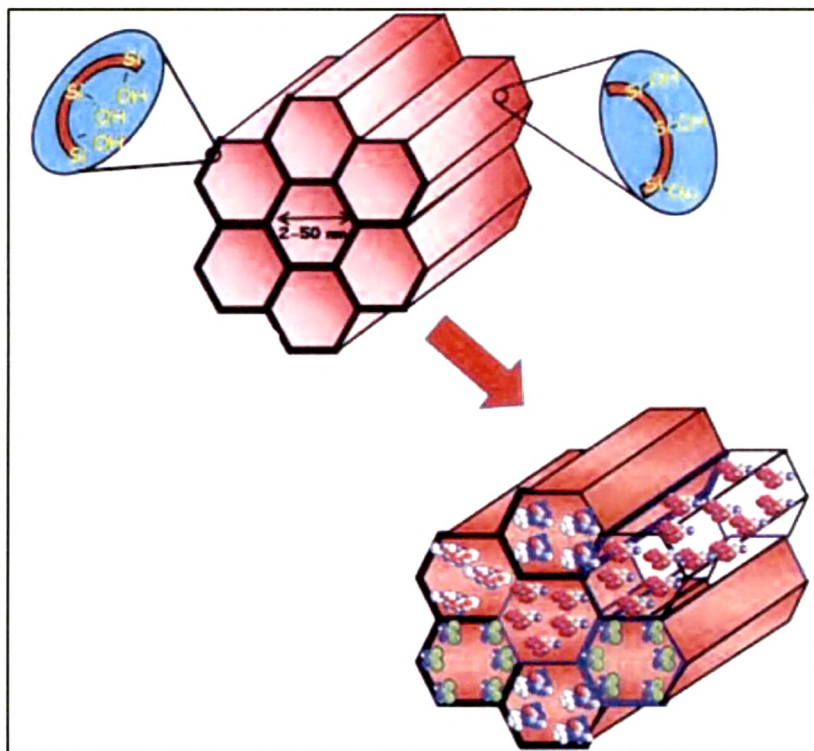
Figure 5.8: Textural properties and drug loading and/or adsorption on MSNs

The probable mechanism of drug loading is that, the a carboxylic acid group of MTX would form hydrogen bonds with the silanol groups of MCM-41 MSNs and consequently drug molecules would be retained into the mesopores[11, 13] (Fig. 5.9).
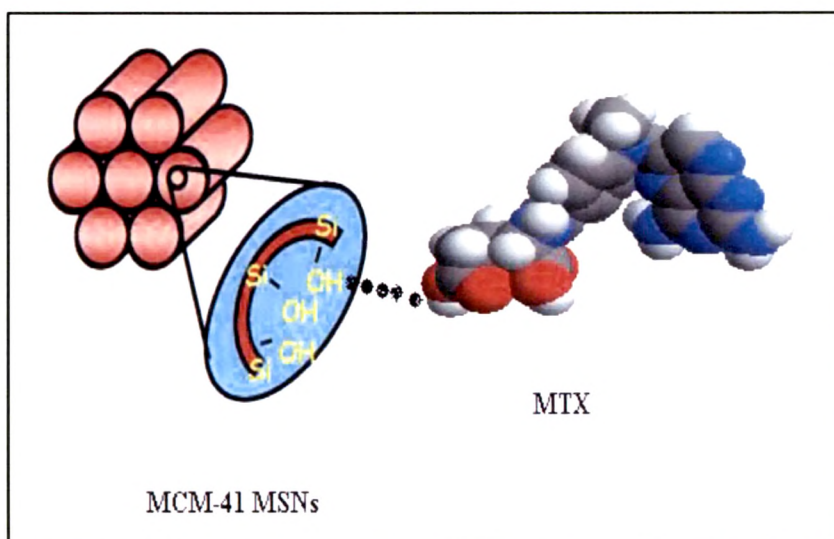
Figure 5.9: MTX linkage to silanol group of MCM-41 MSNs

The drug loading process was also optimized for solvent, ratio of drug and drug carrier (MSNs), temperature, time and stirring rate.

5.6.1 Optimization of drug loading procedure
□*Solvent*

Drug loading into porous materials is based on adsorption from a solution. One of the most crucial factors affecting the drug loading is the selection of loading solvent. Solvent selection is a demanding task, and no models or rules are established for predicting the loading capacities attainable using different loading solvents.

The first prerequisite for a loading solvent is the sufficient solubility of the drug in it. The optimal solvent for the loading process might not be the one in which the solubility is the highest. It is often a sign of strong attractive interactions between the solvent and the solute[14], and it may cause the solute to prefer staying in the solution phase to adsorption onto the carrier. Another inauspicious situation in drug loading is the competitive adsorption; if the solvent possesses attractive interactions with the adsorbent, it will compete on the adsorption sites with the solute. Besides the affinities among the solute, solvents and adsorbent surface, the possible degradation of the API (active pharmaceutical ingredient) in the solvent must also be taken into account. The API may decompose or it may re-crystallize from the solution as a different polymorph/ solvate[10]. Solvents that induce the degradation of the API must be avoided. In addition, the use of many solvents is limited by their toxicity or too low or too high volatility.

For the present study three solvents were tried. As MTX is soluble in solutions of mineral acids and in dilute solutions of alkali hydroxides, 0.1 M HCl and 0.1 M NaOH were selected as solvents. Dimethyl formamide was another solvent checked for drug loading. Drug loading was carried out with these selected solvents and % LE was checked. The results are shown in Table 5.2 and Fig. 5.10.

Table 5.2: Effects of different solvents on MCM-41 MSNs drug loading

Solvent used for drug loading	pH of the medium	% Drug loading in MCM-41 MSNs
Dimethyl formamide	6.8	42. 203
0.1 M HCl	1.2	47. 549
0.1 M NaOH	12.5	13. 220

Results suggest that the drug loading is maximum when 0.1 M HCl was used as a solvent. Optimizations of solvents also cover the optimization of pH for the

loading process. The data of loading process suggested that acidic media is more suitable for effective entrapment of MTX in MCM-41 MSNs.
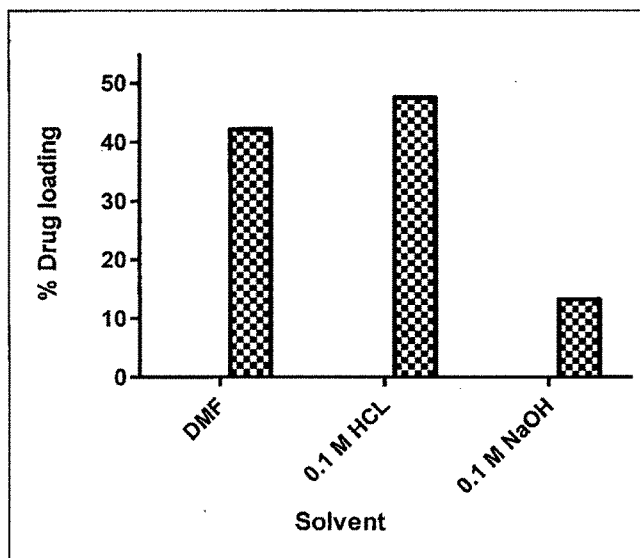
Figure 5.10: Effects of different solvents on MCM-41 MSNs drug loading

☐ *Ratio of drug and drug carrier*

Weight ratio of drug to MSNs can greatly affect drug loading ability. It was necessary to find out the optimum drug to MSNs ratio. To optimize the ratio, different proportion of MSNs to drug was taken as mentioned in Table 5.3.

Table 5.3: Effects of drug: MSNs ratio on MCM-41 MSNs drug loading

Weight ratio Drug :Carrier	% Drug loading in MCM-41 MSNs
1: 0.5	12. 607
1:1	47. 515
1: 1.5	35. 253
1: 2	28. 572

Ratio was optimized by taking fixed proportion of drug and variable proportion of MSNs. Four different drug: MSNs proportions were tested i.e. 0.5, 1, 1.5, and 2. It was found that maximum drug entrapment was achieved with 1:1 weight ratio. The optimization data graphically present in Fig. 5.11.
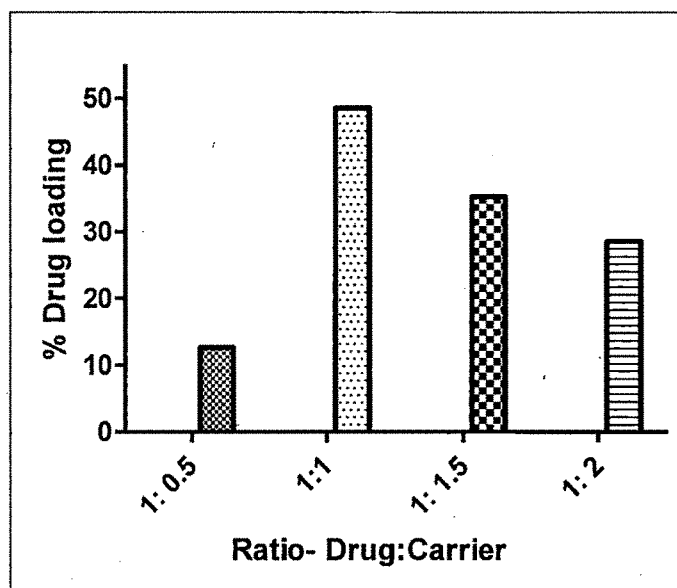
Figure 5.11: Effects of drug:MSNs ratio on MCM-41 MSNs drug loading

☐ *Temperature and time*

• Solubility is a function of temperature. By increasing the loading temperature, the solubility of a drug can be increased. Increase in temperature may also accelerate the degradation of drug or evaporation of the solvent, and the temperature also affects the adsorption rate and equilibrium. On the other hand it is necessary to check the effect of time so loading process was conducted at different time duration.

The loading process was carried out at two different temperature i.e. room temperature and 40°C. Similarly five different time durations were selected for proper agitation during the loading process. Stirring was provided with magnetic stirrer for five different time duration, i.e. 6h, 12h, 24h, 48h, and 72h. The results are summarized in Table 5.4 and Fig. 5.12.

Table 5.4 : Effects of temperature and time on MCM-41 MSNs drug loading

Temperature	% of Drug loading at different time duration				
	6h	12h	24h	48h	72h
Room temp.	40. 965	45. 106	47. 381	46. 240	42. 150
40° C	35. 659	37. 581	39. 162	42. 857	42. 352
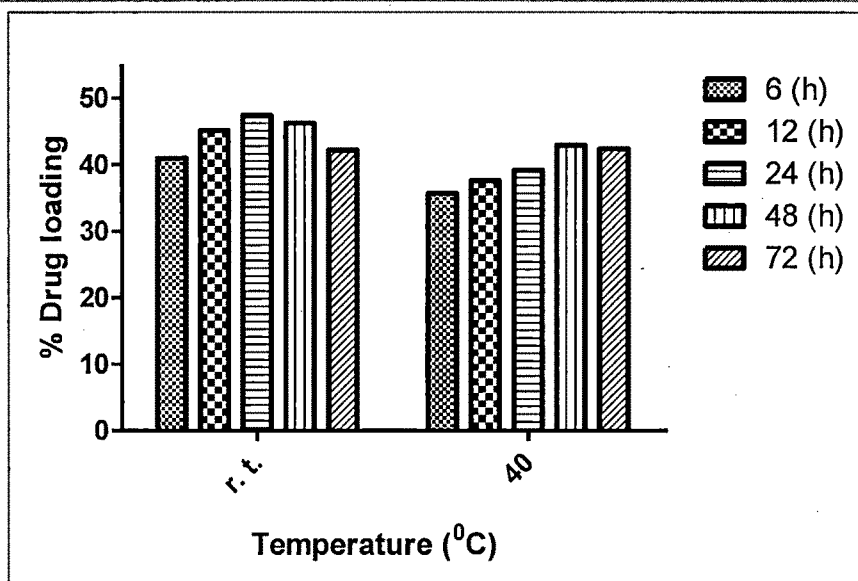
Figure 5.12: Effects of temperature and time on MCM-41 MSNs drug loading

The results of % LE revealed that maximum drug loading was attainable if the MSNs and MTX were continuously agitated for 24h.

The results of drug loading at 40° C suggested that the elevated temperature was not suitable for the high loading. Higher temperature may increase the MTX solubilization but at elevated temperature the MTX molecules may experience high Brownian motion[15-17] which may not allow the easy diffusion and adsorption in the mesopores of MCM-41 MSNs. When drug was loaded at 40° C, it was found that MTX was crystallized out from the solution. The crystallized MTX was not adsorbed into the pores but gets deposited on the surface of MSNs. The deposited MTX is easily removed during the washing of MCM-41 MSNs and leads to poor drug loading.

□*Stirring rate*
During the loading process, the solution is continuously stirred using magnetic stirrer to improve access of the concentrated solution to the mesopores[17]. MSNs sample was added in drug solution with vigorous stirring and vigorous stirring was continued for 1h, followed by gentle stirring for 23h.

Vigorous stirring increases the mechanical shear that result in rapid dispersion of MSNs molecules (in drug solution). Proper dispersion of MSNs in drug solution decreases the chances of agglomerate formation and facilitates the diffusion of drug molecules in the mesopores. Continuous vigorous shaking cause obstacle for drug molecules for their easy diffusion and adsorption to the mesopores. Initial vigorous stirring helps to form fine and uniform dispersion of

MSNs in drug solution, followed by gentle stirring which may help in easy diffusion of drug in to the mesopores, leading to higher drug loading.

Vigorous stirring was provided at 800 rpm, whereas the gentle stirring rate was optimized at four levels i.e. 50 rpm, 100 rpm, 200 rpm and 400 rpm. The results are summarized in Table 5.5 and Fig. 5.13. The results revealed that as stirring rate was increased from 100 rpm to 400 rpm; the rate of drug loading was deceased from 47 to 27 %. Optimized stirring rate data suggested that for the maximum drug loading the stirring should be 100 rpm.

Table 5.5: Effects of stirring rate on MCM-41 MSNs drug loading

Stirring speed	~50 rpm	~100 rpm	~200 rpm	~400 rpm
% Drug loading	45. 658	47. 240	32. 268	27.392
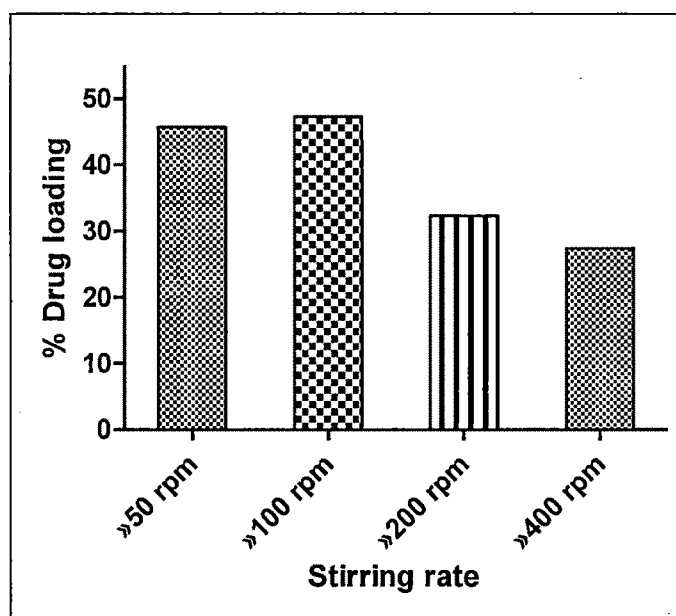
Figure 5.13: Effects of stirring rate on MCM-41 MSNs drug loading

5.6.2 Factorial design for drug loading optimization
The process of drug loading was optimized with respect to different influencing variables such as solvent, ratio of drug: carrier, temperature, time, and stirring rate. The conventional method of optimization involves the study of effect of different factors on formulation by changing one variable at a time (OVAT). Since the combined effects of variables are not evaluated, it is difficult to formulate an ideal pharmaceutical formulation. It is necessary therefore to understand the complexity of process variables in development of pharmaceutical formulations

using statistical analysis of each variable at a time such as factorial design[18]. Factorial designs involve the study of all the selected factors in all possible combinations, in a most efficient manner using minimum experiments. The effect of individual variable can be visualize with the contour plots and is very helpful to evaluate the response of different variables in optimization process. Similarly three-dimensional response surface plots provide platform to study the effect of dependent and independent variables in formulation development.

Primary optimization data revealed that the stirring rate and ratio of drug: MSNs greatly affect the loading efficiency. A statistical model was developed to study the effect of stirring rate, weight ratio of drug:carrier and concentration of drug solution on formulation characteristics.

5.6.2.1 Preparation of batches and optimization by factorial design

Twenty seven batches of MTX loaded MCM-41 MSNs (as a carrier) were prepared using 3^3 factorial design by varying three independent variables the concentration of drug solution (X1), the stirring rate (X2), and drug:carrier ratio (X3). Each factor was tested at three levels of low, medium and high designed as -1, 0, and +1 respectively. The normalized factor levels of independent variables are given in Table 5.6.

Table 5.6: Factorial 3^3: factors, their levels, and transformed values

Variables with transformed value	Levels		
	Low (-1)	Medium (0)	High (1)
(X1) Concentration of drug solution (mg/ml)	1	5	10
(X2) Stirring rate (rpm)	10	50	100
(X3) Ratio drug: carrier	0.25	0.5	1

The % MTX loading efficiency (response variable) of the prepared batches was determined (Table 5.7) and the highest percent drug loading achieved in MCM- 41 MSNs was 47.85% at 1 level of X1 (10 mg/ml), 1 level of X2 (100 rpm), and 1 level of X3 (1:1 weight ratio). The results were subjected to multiple-regression analysis. The fitted equation related to percent loading efficiency and transformed factors is given in Eq. (1).

$$Y= 12.395+ 12.379X1+ 7.146X2+ 5.338X3+ 4.526X12+ 0.844X22+ 2.232X32+$$

$$2.559X1X2+ 3.518X1X3- 0.609X2X3- 2.003X1X2X3$$

(1)

Table 5.7: Different batches with their experimental coded level of variables for 3^3 factorial design

Batch code	X1= Concentration of drug solution	X2= Stirring rate	X3= Ratio drug:carrier	% drug loading
M1	-1	-1	-1	1.901
M2	-1	-1	0	2.183
M3	-1	-1	1	2.832
M4	-1	0	-1	2.086
M5	-1	0	0	6.382
M6	-1	0	1	8.186
M7	-1	1	-1	9.853
M8	-1	1	0	12.303
M9	-1	1	1	13.615
M10	0	-1	-1	4.664
M11	0	-1	0	5.706
M12	0	-1	1	8.315
M13	0	0	-1	12.308
M14	0	0	0	18.318
M15	0	0	1	21.816
M16	0	1	-1	16.606
M17	0	1	0	18.973
M18	0	1	1	23.312
M19	1	-1	-1	14.714
M20	1	-1	0	16.117
M21	1	-1	1	38.961
M22	1	0	-1	19.403
M23	1	0	0	21.101
M24	1	0	1	42.51
M25	1	1	-1	37.807
M26	1	1	0	42.701
M27	1	1	1	47.856

The data indicated that percent loading efficiency is more dependent on the concentration of drug solution and the stirring rate than the ratio of drug:carrier. The value of correlation coefficient (r) was found to be 0.963, indicating a good fit. The small values of coefficients of terms $X2^2$, $X3^2$, X1X2, X2X3,and X1X2X3 (Eq. 2), were least contributing in loading of MTX in MCM-41 MSNs (p>0.05). Hence, they were omitted to evolve the reduced model (Eq. 2). The summary of regression analysis is shown in Table 5.8.

$$Y = 14.446 + 12.379X1 + 7.146X2 + 5.338X3 + 4.526X1^2 + 3.518X1X3 \quad (2)$$

The positive sign for the coefficient of X1, X2, and X3 in Eq. (2) showed that the percent drug loading can be increased by an increase in X1, X2, and X3. The results of ANOVA of the second-order polynomial equation are given in Table 5.8.

Table 5.8: Analysis of variance (ANOVA) of variables for full and reduced model of MCM-41 MSNs

	DF	SS	MS	F	R	R^2	Adj.R^2
Regression							
FM	10	4511.708	451.170	17.707	0.957	0.917	0.865
RM	5	4362.338	872.467	37.128	0.947	0.898	0.874
Error							
FM	16	344.105	21.506				
RM	21	493.475	23.498				

[SSE2–SSE1 = 493.475– 344.105= 149.3697788
No. of parameters omitted = 5
MS of error (full model) = 21.506
F calculated = (SSE2–SSE1/no. of parameters omitted)/MS of error (full model)
= (149.369/5)/21.506 = 1.389
Tabled F value = 2.85 (α = 0.05, V1 = 5, and V2 = 16).
a Where DF indicates degrees of freedom; SS sum of square; MS mean sum of square and F is Fischer's ratio].

F-Statistic of the results of ANOVA of full and reduced model confirmed omission of non-significant terms of Eq. (1) and (2). Since the calculated F value (1.389) was less than the tabled F value (2.85), it was concluded that the neglected terms do not significantly contribute in the prediction.

The goodness of fit of the model was checked by the determination coefficient (R^2). In this case, the values of the determination coefficients (R^2) and adjusted determination coefficients (adj R^2) were very high (>85%), which indicates a significance of the model. All the above considerations indicate an adequacy of the regression model[19, 20].

5.6.2.2 Contour plots

Figure 5.14 (a–i) is the contour plot for MCM-41 MSNs which were found to be linear and signifying linear relationship between variables X1, X2, and X3. It was observed from contour plots (Fig. 1c) that maximum LE (47.856%) could be obtained with X2 between 0.5 level (50 rpm) to 1 level (100 rpm) and X3 between 0.5 level (0.5:1) to 1 level (1:1). Fig. 1f revealed that maximum loading could be obtained with X1 between 0.4 level (6 mg) to 1 level (10 mg) and X3 between 0.5

level (0.5:1) to 1 level (1:1). Fig. 1i showed that maximum loading could be obtained with X1 between 0.6 level (6 mg) to 1 level (10 mg) and X2 between 0.5 level (50 rpm) to 1 level (100 rpm). All the two-dimensional contour plots were found to follow the linear relationship between X1, X2, and X3 variables. From the contour, it was observed that higher drug concentration (10 mg/ml), maximum stirring rate (100 rpm), and unit ratio of drug:carrier are necessary for maximum drug loading.
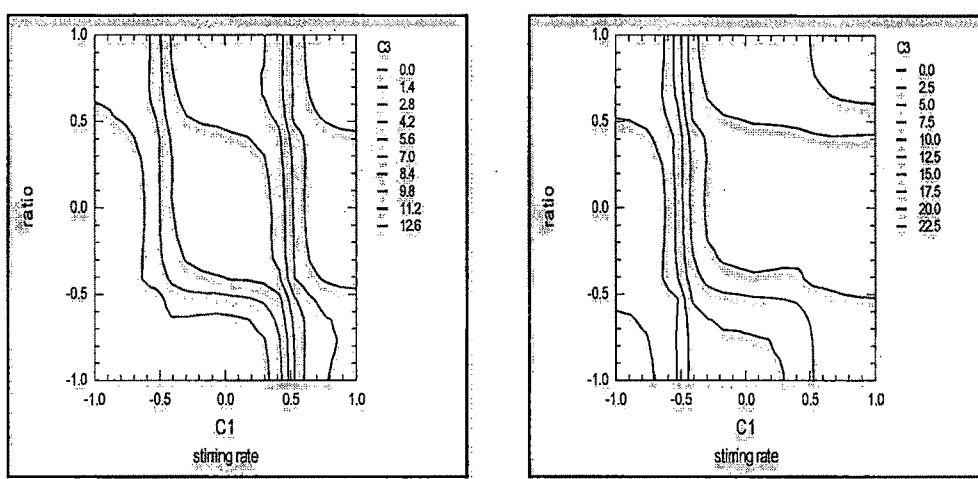
(a) Effect on LE at -1 level of X1

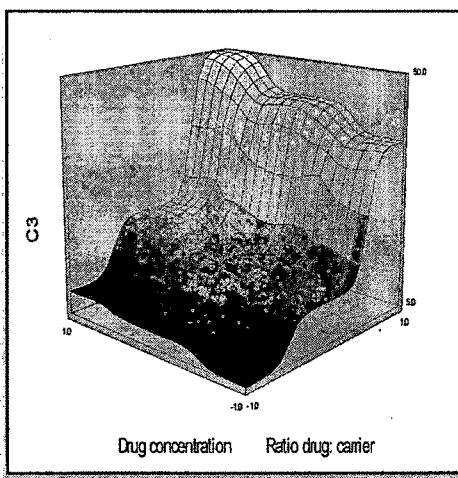(b) Effect on LE at 0 level of X1
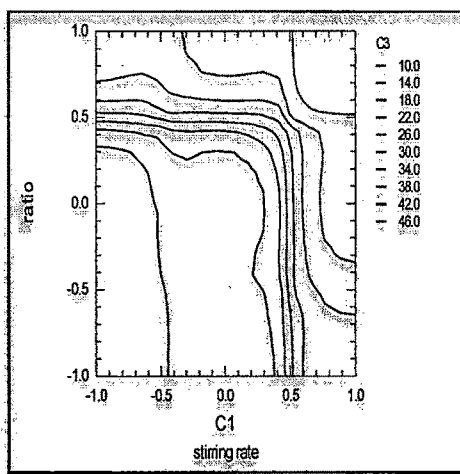
(c) Effect on LE at +1 level of X1

Figure 5.14: Contour plots: Effect on LE at -1, 0 and +1 levels of drug concentration (X1)
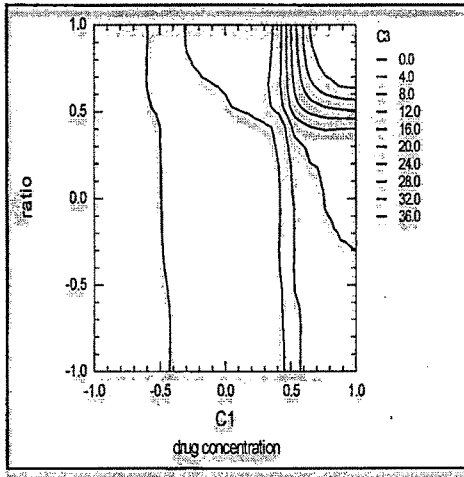
(d) Effect on LE at -1 level of X2
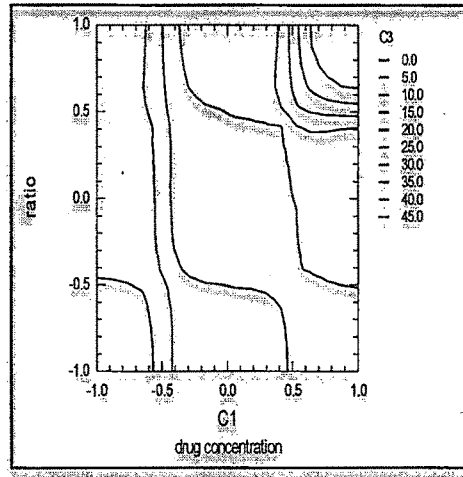
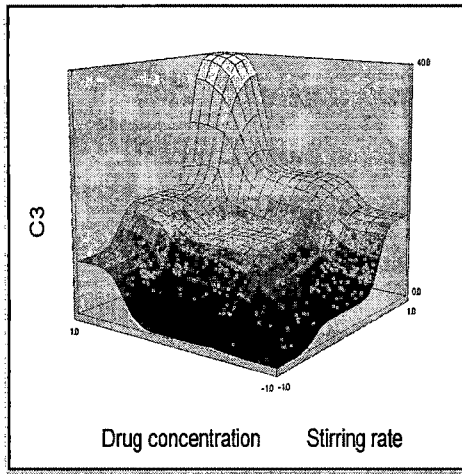(e) Effect on LE at 0 level of X2
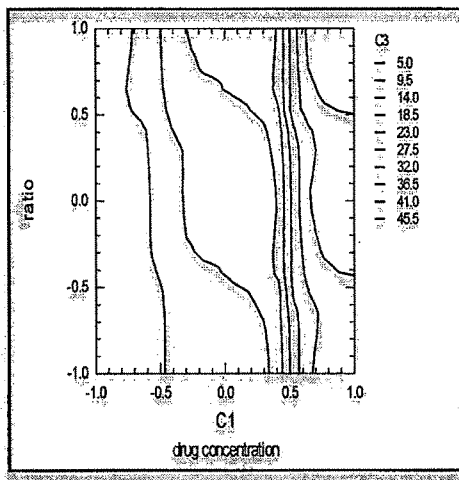
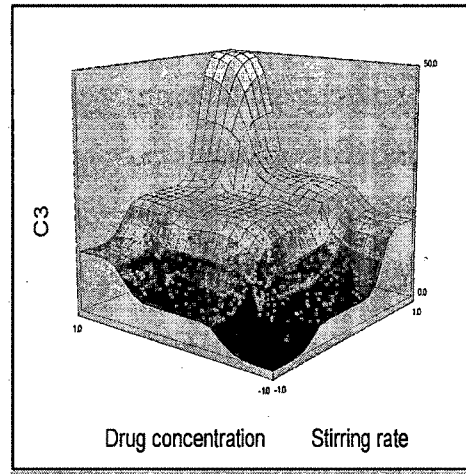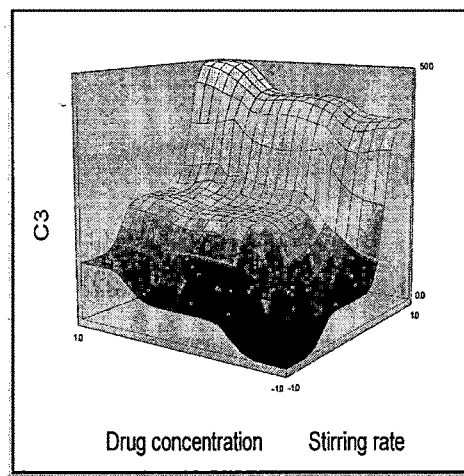
(f) Effect on LE at +1 level of X2

Figure 5.14: Contour plots: Effect on LE at -1, 0 and +1 levels of stirring rate (X2)
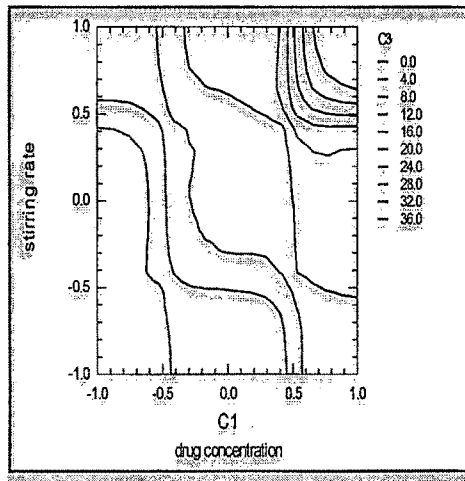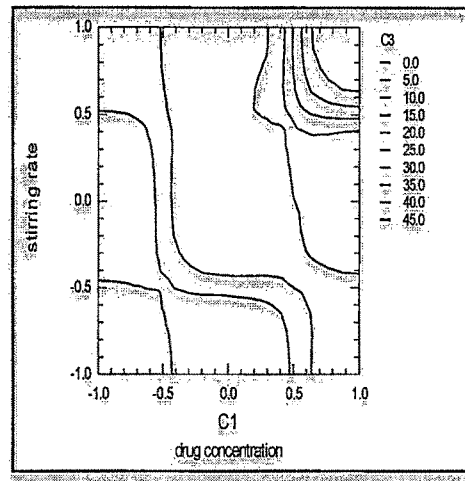
(g) Effect on LE at -1 level of X3   (h) Effect on LE at 0 level of X3
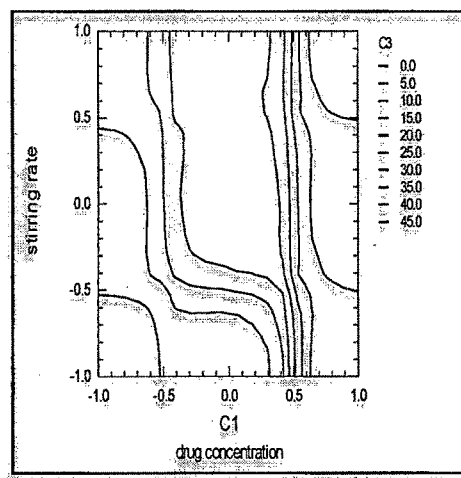
(i) Effect on LE at +1 level of X3

Figure 5.14: Contour plots: Effect on LE at -1, 0 and +1 level of drug: carrier ratio (X3)

5.6.2.3 Response surface plots

Three dimensional response surface plots generated by the NCSS software are presented in Fig. 5.15 (a-i), for MCM- 41 MSNs. Fig. (a-c) depict response surface plots for LE of MCM-41 MSNs at constant level of the factor X1 showing an increase in LE with increase in the stirring rate and increase in weight ratio of drug:carrier. Fig. (d-f) depict response surface plots for LE at constant level of the factor X2 indicating an increase in LE with increase in the drug concentration and

121

increase in weight ratio of drug:carrier. Fig. (g-i) depict response surface plots for LE at constant level of the factor X3 which suggesting an increase in drug concentration and increase in stirring rate increases the LE.
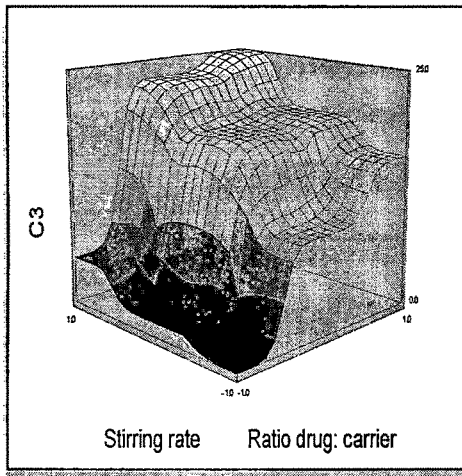
(a) Effect on LE at -1 level of X1
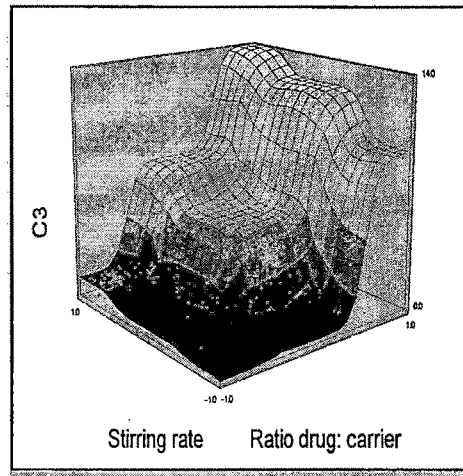
(b) Effect on LE at 0 level of X1
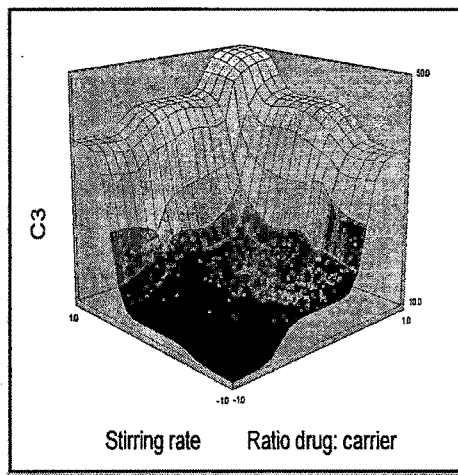
(c) Effect on LE at +1 level of X1

Figure 5.15: Response surface plots: Effect on LE at -1, 0 and +1 level of drug concentration (X1)
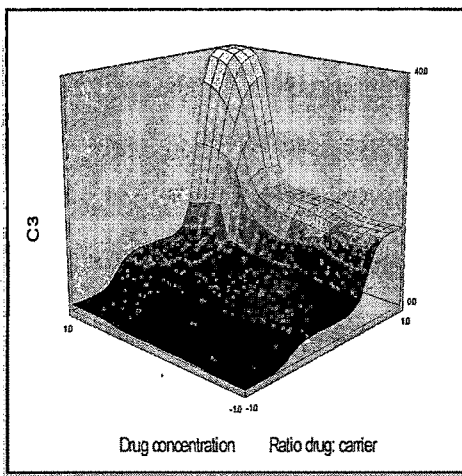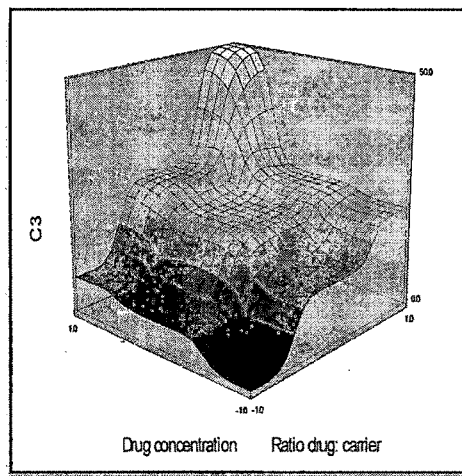
(d) Effect on LE at -1 level of X2   (e) Effect on LE at 0 level of X2

(d) Effect on LE at +1 level of X2

Figure 5.15: Response surface plots: Effect on LE at -1, 0 and +1 level of stirring rate (X2)

(g) Effect on LE at -1 level of X3

(h) Effect on LE at 0 level of X3

(g) Effect on LE at +1 level of X3

Figure 5.15: Response surface plots: Effect on LE at -1, 0 and +1 level of drug: carrier ratio(X3)

5.6.3 Evaluation of drug loaded MCM-41 MSNs

Drug loaded MSNs were evaluated for maximum drug loading and intact mesoporosity. Different instrumental techniques like TEM, XRD, nitrogen adsorption, FTIR and DSC were used for this purpose.

5.6.3.1 Transmission electron microscopy (TEM)

The first step was to check that the mesostructure of the MCM-41 MSNs has survived after the loading process. The MSNs sample was analyzed by TEM. The high resolution TEM images confirmed the prevalence of the ordered mesostructure after the loading step (Fig. 5.16). TEM Images are marked with some dark spots, which may be the indicative of the confinement of drug molecules within the pores.
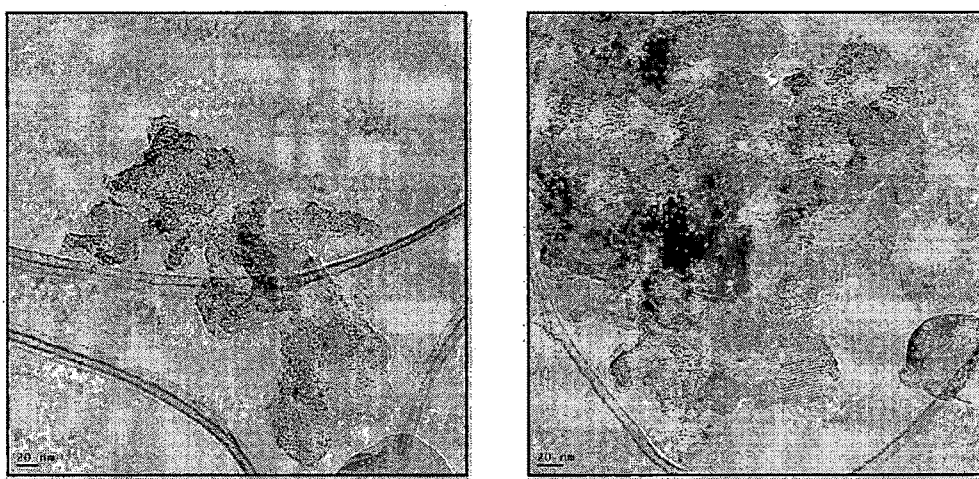
Figure 5.16: TEM images of MSNs after drug loading

5.6.3.2 Powder X-ray diffraction (XRD)

The survival of mesoporosity of the MSNs was further confirmed by XRD. For this purpose, a small angle XRD pattern was carried out before and after the loading process (Fig. 5.17 and 5.18). The mesoporous structure of the MSNs was confirmed by the diffraction peaks at 100, 110 and 200. The same characteristic diffraction peaks were observed in MSNs even after the drug loading process. The presence of peaks was indicated that the mesostructure of MSNs was not disturbed after the drug loading. The XRD pattern of MTX is also shown in Fig. 5.18. The drug loaded MSNs show lack of MTX characteristic peaks in XRD pattern further confirming the entrapment of drug molecules within the mesopores.

5.6.3.3 Nitrogen adsorption isotherm (BET surface analysis)

After the confirmation of the integrity of the mesostructure, next important point was to check whether the drug molecules are confined inside the mesopores or they are just on the outer surface of the MSNs. Nitrogen adsorption analysis was performed to find out the status of drug molecules. The nitrogen adsorption isotherms were obtained for the pore size distribution and the pore volume determination of MSNs, before and after the loading process.
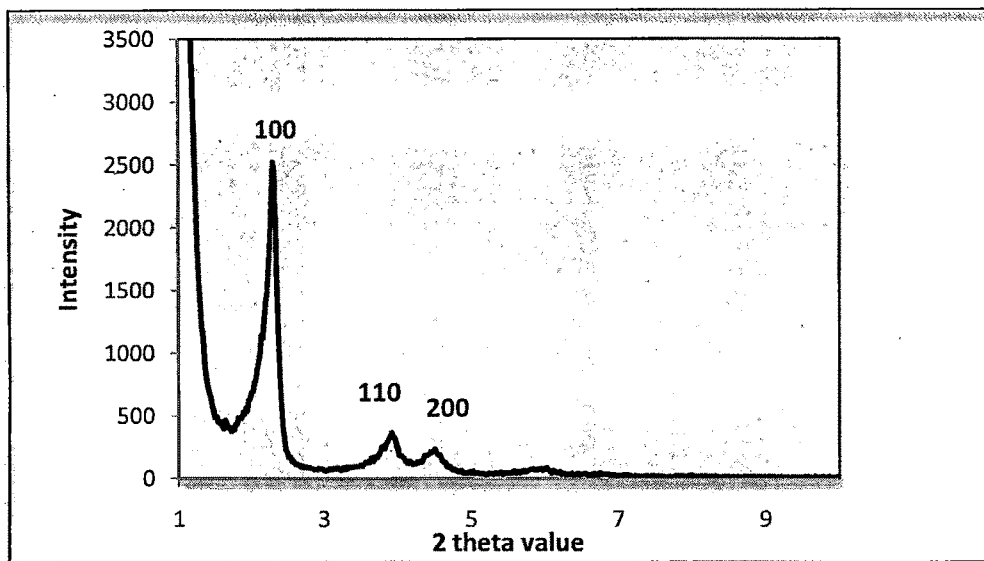
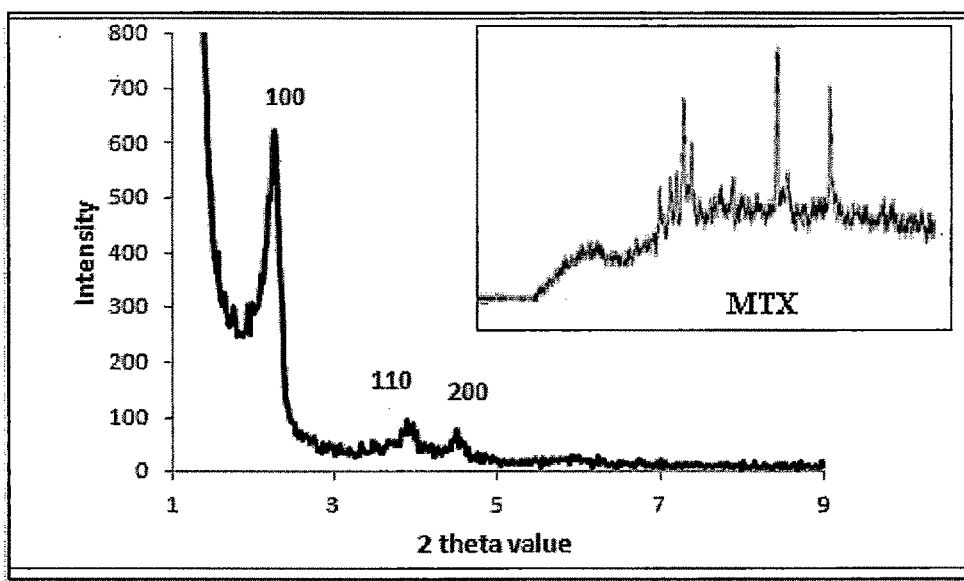**Figure 5.17: XRD pattern of MCM-41 MSNs before the drug loading**

Figure 5.18: XRD pattern of MTX and MCM-41 MSNs after the drug loading

126

The pore volume and surface area are normally decreased as a consequence of the MSNs–drug interaction. It can be noted from Fig. 5.20 and 5.21 that the available pore volume was decreased after the drug loading. Decrease in pore volume suggested that the drug molecules are partially filling the mesopores, i.e. the drug molecules are being confined inside the pores[21].

In Fig. 5.19 and 5.20 nitrogen adsorption-desorption isotherms of MCM-41 MSNs before and after the drug loading were reported. Both the isotherm of MCM-41 MSNs shows typical type IV isotherm according to IUPAC classification represents the mesoporosity. The isotherm recorded for MCM-41 MSNs also shows a hysteresis loop at high relative pressure, which has been ascribed to the presence of interparticle porosity[5, 10].
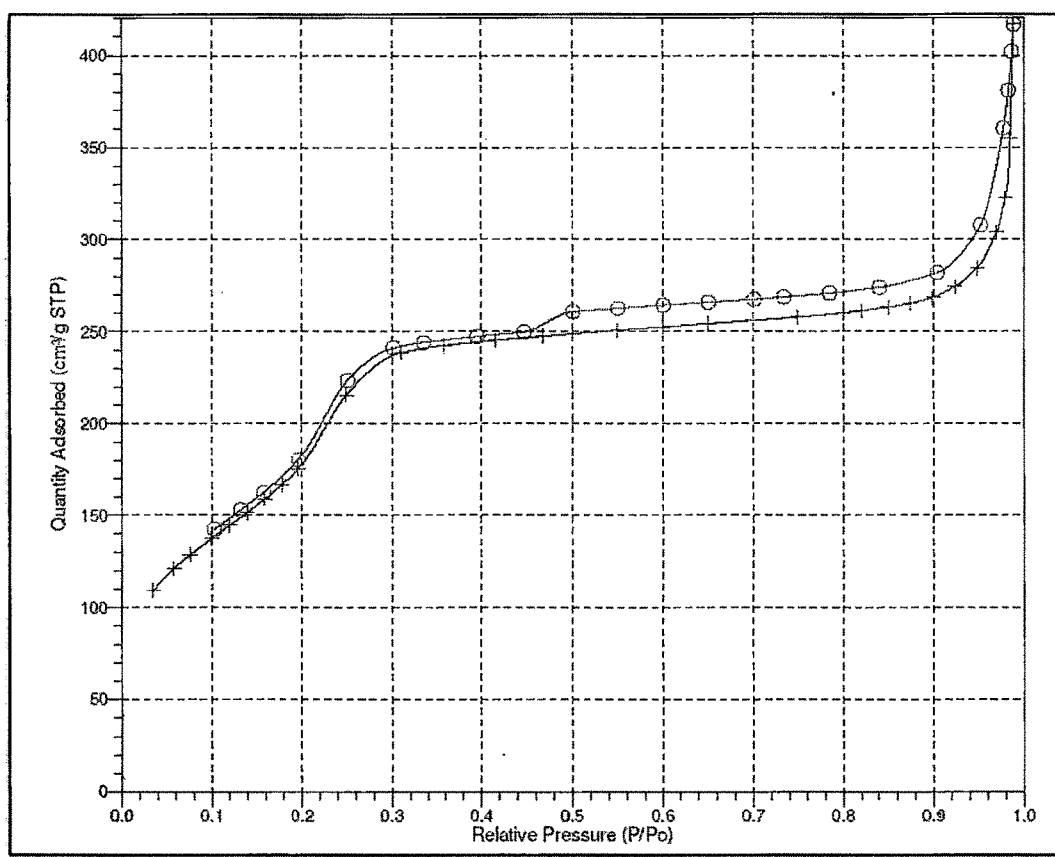
Figure 5.19: Nitrogen adsorption isotherm of MCM-41 MSNs before the drug loading

The calculated B.E.T. specific surface area for MCM-41 MSNs alone and MCM-41 MSNs after MTX loading were found to be 739.673 and 307.204 m²/g, respectively. The adsorption isotherms of MTX loaded MSNs showed that the adsorbed nitrogen volume decreased after drug loading. Correspondingly, the average pore

size distribution for drug loaded MCM-41 MSNs, calculated by the BJH–KJS method, was shifted from 3.69 nm to 2.95 nm and the mesopore volume decreased from 0.470 to 0.229 cm^3/g for the primitive MCM-41 MSNs and drug loaded MCM- 41 MSNs, respectively (Fig. 5.21). Numerical data are shown in Table 5.9 for MCM-41 MSNs and drug loaded MCM-41 MSNs.
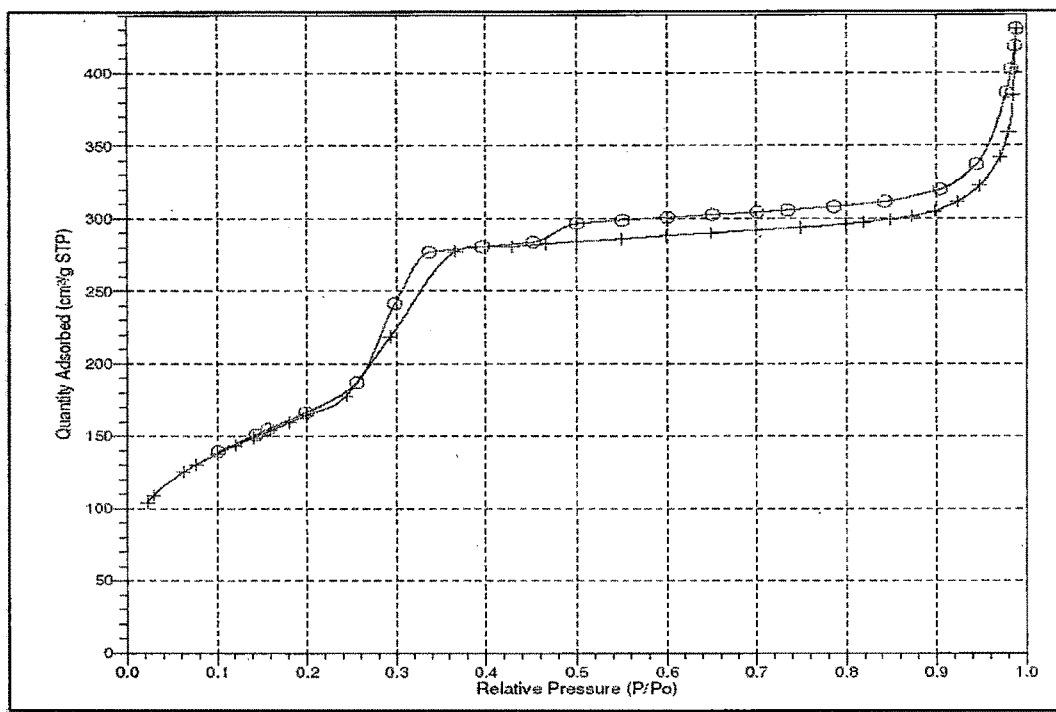

Figure 5.20: Nitrogen adsorption isotherm of MCM-41 MSNs after the drug loading

Table 5.9: Pore diameter, volume and BET surface area of MCM-41 MSN

MSNs	Pore diameter (nm)	Pore volume (cm^3/g)	S_{BET} (m^2/g)
MCM-41	3.696	0.470	739.671
MTX loaded MCM-41	2.952	0.229	307.204
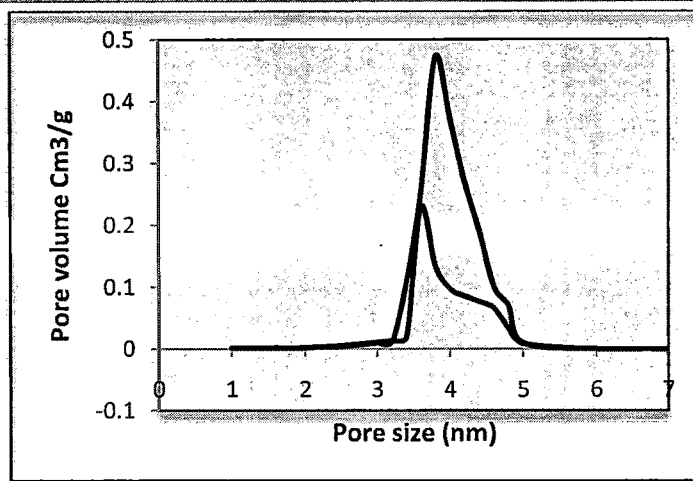
Figure 5.21: Pore size distribution and pore volume of MCM-41 MSN before and after drug loading

5.6.3.4 FTIR analysis

FTIR spectrum of MCM-41 MSNs (Fig. 5.23) showed the presence of a vibration band at 3740 cm^{-1} attributable to isolated terminal silanol groups and of another large band at 3611 cm^{-1} attributable to geminal and associated terminal silanol groups. The stretching vibrations of Si-O-Si and Si-OH can be seen at 1070 and 958 cm^{-1}. The FTIR spectral analysis of MTX powder (Fig. 5.22) showed the principal peaks at about 1682 cm^{-1} (– COOH), 1639 cm^{-1} (– CO-NH), 1541, 1489 cm^{-1} (aryl system), and 825 cm^{-1} (aromatic ring system) confirming the purity of the drug. The spectra of drug loaded MCM-41 MSNs (Fig. 5.24) shows a remarkable absence of the peak as it observes in MTX pure sample, suggest that majority of MTX was entrapped in MSNs.
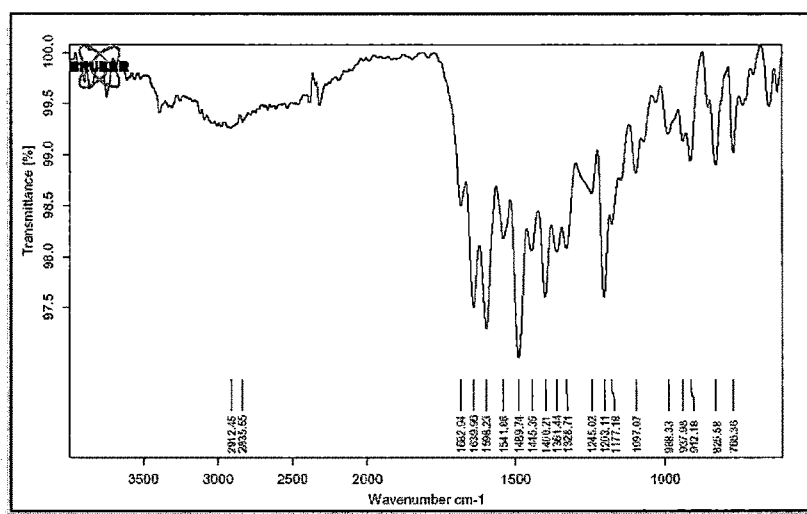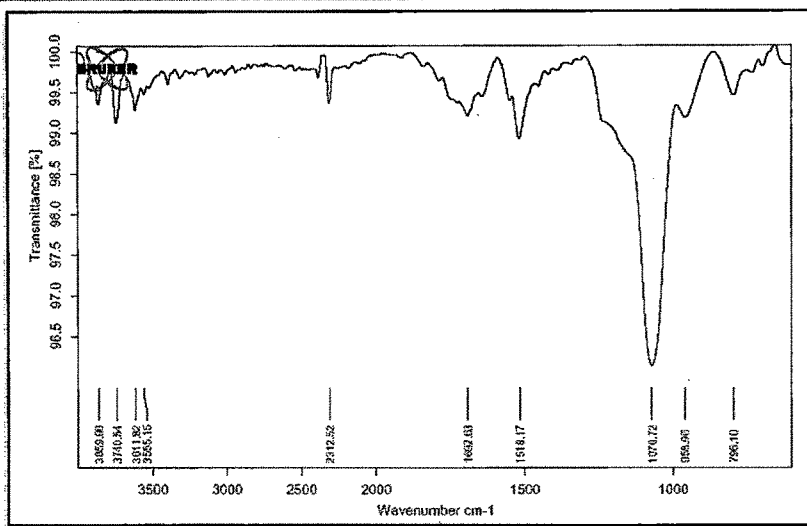

Figure 5.22: FTIR spectra of MTX

129

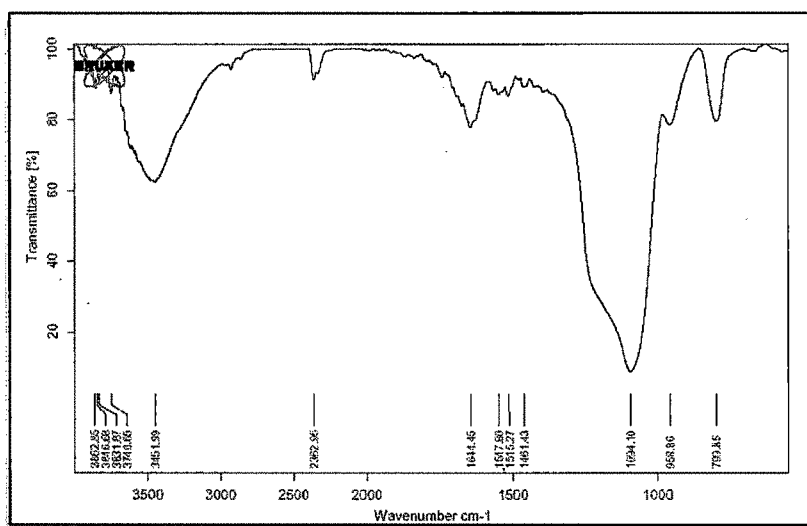**Figure 5.23: FTIR spectra of MCM-41 MSNs**

Figure 5.24: FTIR spectra of MTX loaded MCM-41 MSNs

5.6.3.5 Differential scanning calorimetry (DSC)

Thermal method like DSC is essential tool to determine, whether the drug is entrapped within the pores or it is partially crystallized onto the external surface of MSNs. The possible surface fraction can be detected using DSC, which detects all the reactions and phase transitions which are associated with enthalpy changes. If any crystalline particles exist on the surface, they appear as a melting endotherm on the DSC scan. The absence of endothermic peak in drug loaded MSNs is the indicative of the amorphous state as drug is confined within the pores.
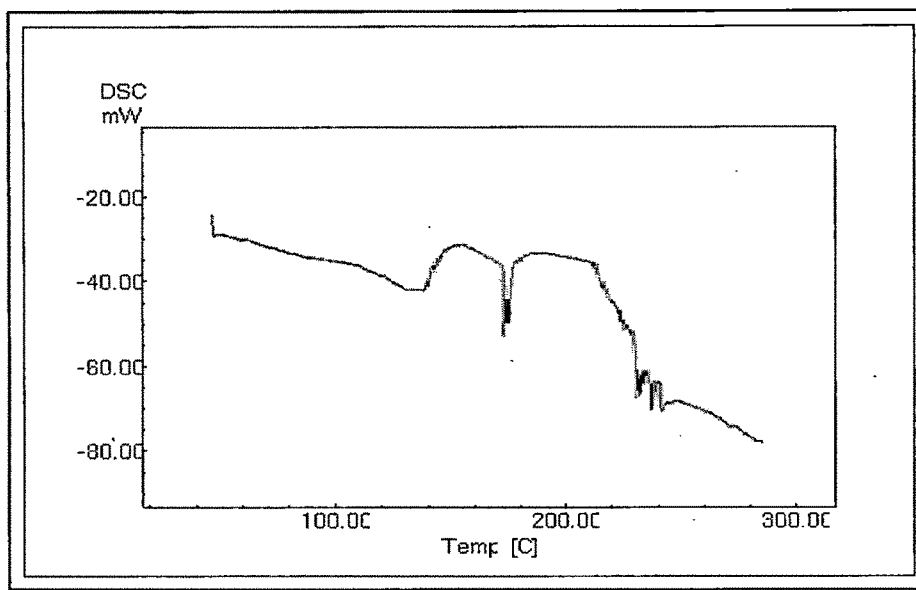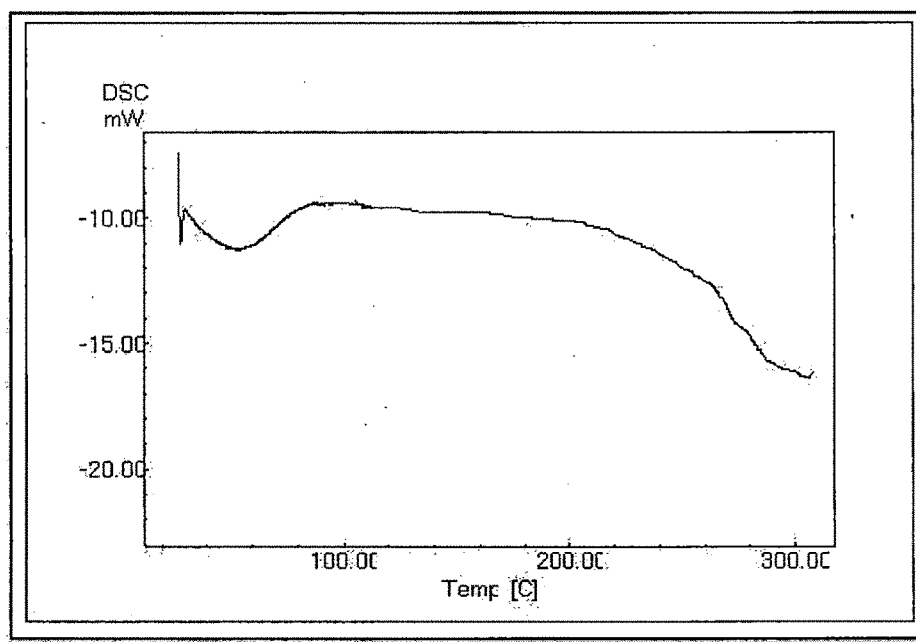
Figure 5.25: DSC thermogram of MTX
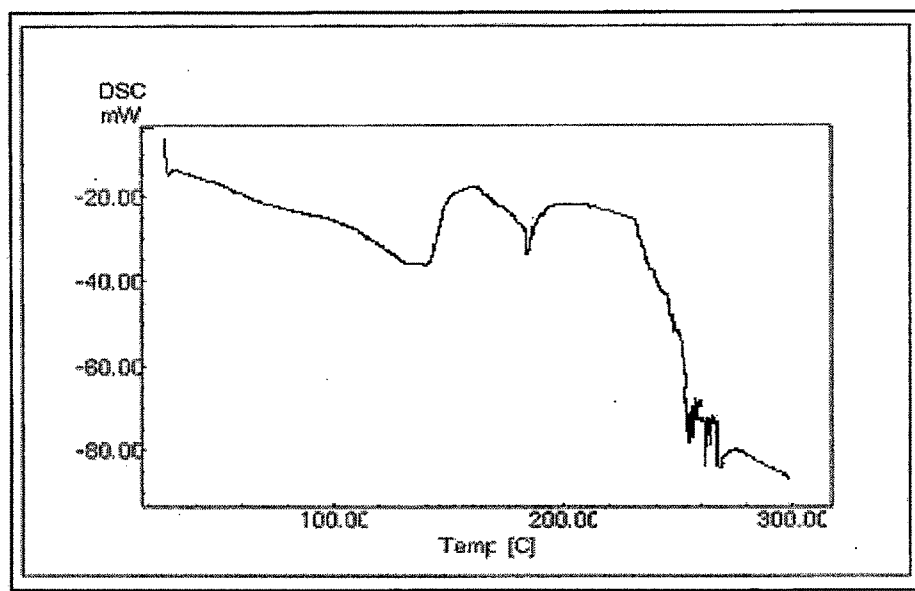

Figure5.26: DSC thermogram of MCM-41 MSNs

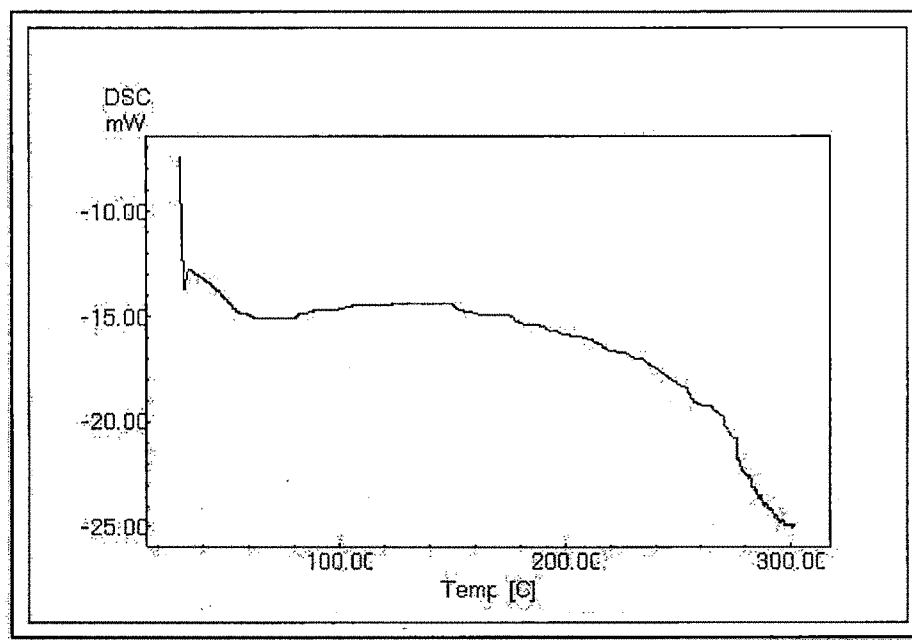**Figure 5.27: DSC thermogram of physical mixture of MTX and MCM-41 MSNs**

Figure 5.28: DSC thermogram of MTX loaded MCM-41 MSNs

Fig. 5.25-5.28 shows DSC thermograms of MCM-41 MSNs, drug loaded MCM-41 MSNs, physical mixture, and crystalline MTX. The DSC curve of MTX exhibits a single endothermic peak at 180 °C, which corresponded to its intrinsic melting points. Physical mixture of drug and MSNs show the less intense peak at 180°C,

indicated that drug molecules are not confined within the pores and drug was present in it crystalline state. However, no melting peak of MTX was identified in the DSC curves obtained from drug loaded MSNs. The absence of phase transitions owing to MTX in the DSC analysis is evidence that MTX is in a non-crystalline state.

5.7 *In-Vitro* dissolution study

Dissolution tests were performed at different pH conditions in order to investigate the drug release behavior in different regions of gastrointestinal tract. MTX dissolution from MCM-41-MTX was compared with those from MTX crystalline powder, physical mixture and marketed formulation (Fig. 5.30, a–d). In all test conditions MTX release from MCM-41 MSNs had a more rapid burst effect than the pure powder, physical mixture and marketed formulation. Schematic presentation of drug release from MCM-41 MSNs was shown in Fig. 5.29.
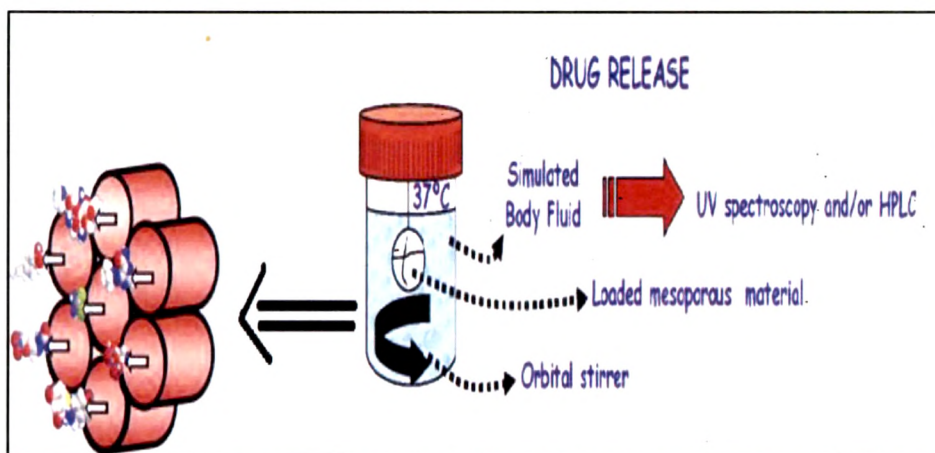

Figure 5.29: Schematic presentation of drug release from MCM-41 MSNs

The dissolution improvement may be largely attributed to the pore channels of the carriers i.e. MCM-41 MSNs, changing the crystalline state of MTX to an amorphous state, which is known to improve the drug solubility and dissolution rate[22-24]. In addition, the particle sizes of the amorphous drug incorporated in the pore channels (nanometer range) were significantly reduced compared with that of pure crystalline MTX (micron range). It is evident that a further decrease in the particle size to the nanometer range will further accelerate the drug release profile and, consequently, improve the dissolution rate[22, 24, 25].

Table 5.10 and 5.11 show the MTX release percentages at the tested pHs after 10 and 30 min respectively. It can be observed that differences in the release profile were more prominent in alkaline fluids. In fact, in pH 7.4 medium more than 60% of drug is released from MCM-41–MTX and a complete drug (100%) release was

obtained after 30 min, whereas MTX dissolution from the crystalline powder was as low as 15% and less than 50% after 10 and 30 min respectively.

Table 5.10: Percentage of drug release after 10 minutes

Dissolution media	% drug release			
	Crystalline drug	Physical mixture	Marketed formulation	Developed formulation
Simulated gastric fluid pH 1.2	4.503	2.903	4.127	5.354
Phosphate buffer pH 4.5	7.869	8.504	10.052	31.443
Phosphate buffer pH 6.8	9.541	11.620	24.636	57.681
Simulated intest. fluid pH 7.4	15.321	17.427	26.320	61.127

Table 5.11: Percentage of drug release after 30 minutes

Dissolution media	% drug release			
	Crystalline drug	Physical mixture	Marketed formulation	Developed formulation
Simulated gastric fluid pH 1.2	38.754	15.546	23.145	74.821
Phosphate buffer pH 4.5	45.723	61.208	71.467	84.760
Phosphate buffer pH 6.8	47.960	79.482	85.511	99.929
Simulated intest. fluid pH 7.4	48.409	79.210	85.124	100.000

Finally, the MTX dissolution profile from MCM-41–MTX at pH 7.4 was compared to that of MTX from commercial formulation. The dissolution profiles indicate that after the 10 min, more than 60% drug was released from MCM-41–MTX whereas only 26% drug was released from the commercial tablet formulation of MTX. Similarly after 30 min drug release from marketed formulation was found to be 85% whereas complete release was obtained from the developed formulation.
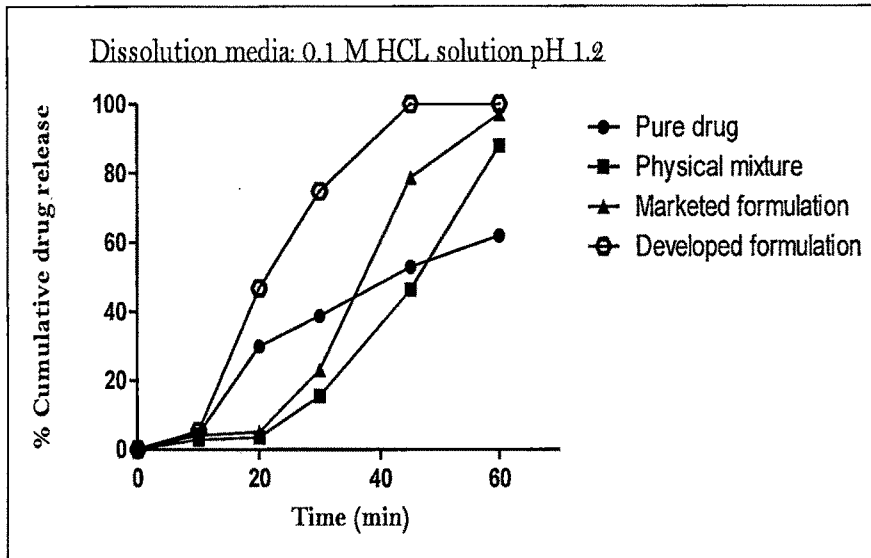
Figure 5.30-a: Release profile of MTX from crystalline MTX, physical mixture, marketed formulation, and developed formulation in pH 1.2
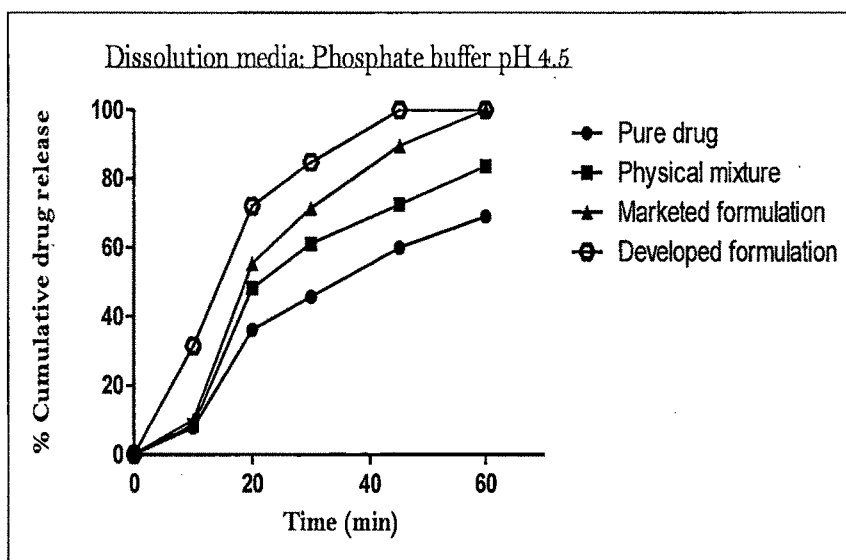

Figure 5.30-b: Release profile of MTX from crystalline MTX, physical mixture, marketed formulation, and developed formulation in pH 4.5
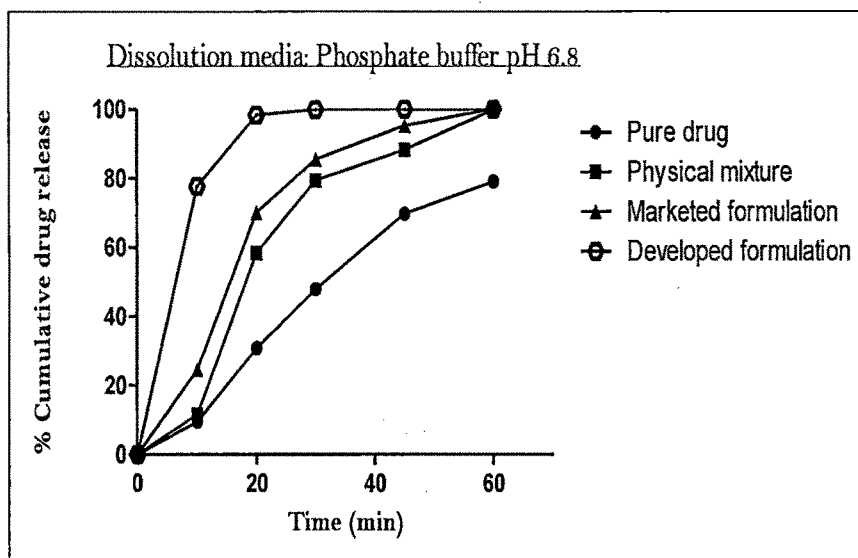
Figure 5.30-c: Release profile of MTX from crystalline MTX, physical mixture, marketed formulation, and developed formulation in pH 6.8
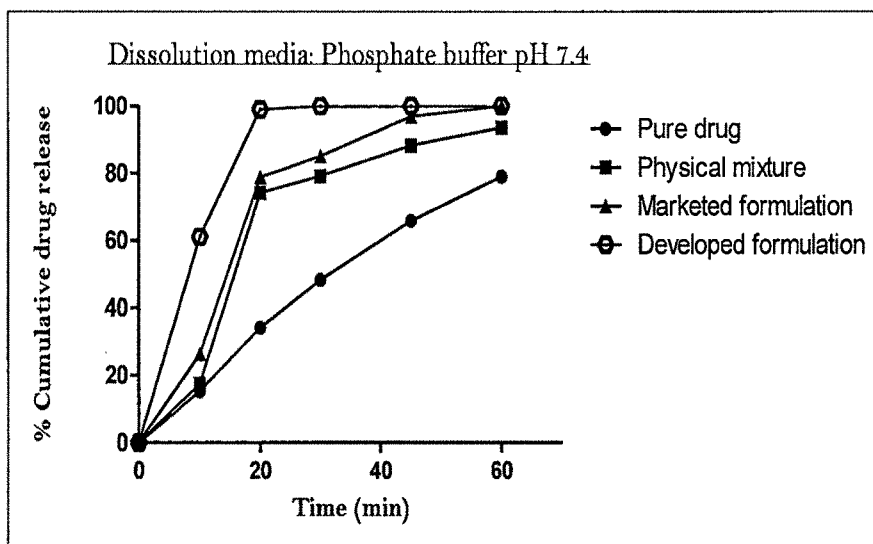

Figure 5.30-d: Release profile of MTX from crystalline MTX, physical mixture, marketed formulation, and developed formulation in pH 7.4

References:

1 Beck JS, Vertuli JC, Roth WJ, Leonowicz ME, Kresge CT, Schmitt KD, Chu C, Olson DH, Sheppard EW, McCullen SB, Higgins JB, Schlenker JL. A new family of mesoporous molecular sieves prepared with liquid crystal templates. J Am Chem Soc 1992; 114: 10834-10843.

2 Kresge CT, Leonowicz ME, Roth WJ, Vartuli JC, U S Patent, 1992; US 5,098,684.

3 Vadia NH, Rajput S. Mesoporous material, MCM-41: A new drug Carrier. Asn J Phar Clic Res. 2011; 4: 44-53.

4 Ghiaci M, Abbaspur A, Kia R, Seyedeyn-Azad F. Equilibrium isotherm studies for the sorption of benzene, toluene, and phenol onto organo-zeolites and as-synthesized MCM-41. Sep Purif Technol. 2004; 40: 217–229.

5 Brunauer S, Emmet P, Teller E. Adsorption of gases in multi molecular layers. J Am Chem Soc. 1938; 60: 309–319.

6 Wujun Xu, Qiang Gao, Yao Xua, Dong Wu, Yuhan Sun, Wanling Shen, Feng Deng. Controllable release of ibuprofen from size-adjustable and surface hydrophobic mesoporous silica spheres. Powd Tech. 2009; 191: 13-20.

7 Ambrogia V, Perioli L, Marmottinib F, Giovagnolia S, Espositoa M, Rossia C. Improvement of dissolution rate of piroxicam by inclusion into MCM-41 mesoporous silicate. Eur J pharm Sci. 2007; 32: 216–222.

8 Ciesla U, Schu¨ th F, 1999. Ordered mesoporous materials. Micropor. Mesopor. Mater. 1999; 27: 131–149.

9 Schulz-Ekloff G, Rathousky J, Zukal A. Controlling of morphology and characterization of pore structure of ordered mesoporous silica. Micropor Mesopor Mater. 1999; 27: 273–285.

10 Choma J, Jaroniec M, Burakiewicz-Mortka W, Kloske M. Critical appraisal of classical methods for determination of mesopore size distributions of MCM-41 materials. Appl Surf Sci. 2002; 196: 216–223.

11 Maria V, Francisco B, Daniel A. Mesoporous materials for drug delivery Angew Chem Int Ed. 2007; 46: 7548–7558.

12 Ida SC, Luigi P, Flaviano T, Rosario A, Francesco P, Francesca I, Nevio P. Silica based mesoporous materials as drug delivery system for methotrexate release. Drug Del. 2007; 14: 491–495.

13 María V, Francisco B, Montserrat C, Miguel M. Drug confinement and delivery in ceramic implants. Drug Met Let. 2007; 1: 37-40.

14 Griesser U.J, The importance of solvates. In Hilfiker R, ed. Polymorphism. Wiley-VCH Verlag GmbH & Co. KGaA, Weinheim, 2006; 211–233.

15 CRC handbook of solubility parameters and other cohesion parameters, A. F. M. Barton, ed., 2nd ed., CRC Press cop, Boca Raton (FL), 1991.

16 Bhattachar SN, Deschenes LA, Wesley JA. Solubility: it's not just for physical

chemists. Drug Dis Today. 2006; 11: 1012–1018.

17   Bennema P, Van J, Van W, Los JH, Meekes H. Solubility of molecular crystals: Polymorphism in the light of solubility theory. Int J Pharm. 2008; 351: 1–2, 74–91.

18   Vandervoort J, Ludwig A. Preparation factors affecting the properties of polylactide nanoparticles: a factorial design study. Pharmazie. 2001; 56: 484– 488.

19   Box G, Hunter W, Hunter J. Statistics for experiments, John Wiley and Sons, New York, 1978; 291–334.

20   Cochran W.G, Cox G.M. Experimental Designs, second ed., John Wiley and Sons, New York, 1992; 335–375.

21   Miguel M, Maria V. New developments in ordered mesoporous materials for drug delivery J Mater Chem. 2010; 20: 5593–5604.

22   Salonen J, Laitinen L, Kaukonen AM, Tuura J, Björkqvist M, Heikkilä T, Vähä-Heikkilä K, Hirvonen J, Lehto V.P. Mesoporous silicon microparticles for oral drug delivery: loading and release of five model drugs. J Control Rel. 2005; 108: 362–374.

23   Heikkilä T, Salonen J, Tuura J, Kumar N, Salmi T, Murzin D.Y, Hamdy M.S, Mul G, Laitinen L, Kaukonen A.M, Hirvonen J, LehtoV. Evaluation of mesoporous TCPSi, MCM-41, SBA-15, and TUD-1 materials as API carriers for oral drug delivery. Drug Deliv. 2007; 14: 337–347.

24   Vasconcelos T, Sarmento B, Costa P. Solid dispersions as strategy to improve oral bioavailability of poor water soluble drugs. Drug Discov Today. 2007; 12: 1068–1075.

25   Kesisoglou F, Panmai S, Wu Y. Nanosizing. Oral formulation development and biopharmaceutical evaluation. Adv Drug Deliv Rev. 2007; 59: 631–644.